负载型 ZrO₂ 催化苯甲醛 Meerwein-Ponndorf-Verley 反应中的载体效应

张　波*, 汤明慧, 袁　剑, 吴　磊

浙江工业大学工业催化研究所, 浙江杭州 310014

摘要: 采用浸渍法制备了 Si-MCM-41 和 Al-MCM-41 (Si/Al = 50) 介孔分子筛, SiO₂, γ-Al₂O₃ 及 MgO 等负载的 ZrO₂ 催化剂, 考察了其在以异丙醇为氢源苯甲醛 Meerwein-Ponndorf-Verley (MPV) 还原反应中的催化活性, 并与纯 ZrO₂ 的催化活性进行对比. 同时, 采用 X 射线衍射、N₂ 吸脱附法、X 射线光电子能谱、紫外-可见漫反射光谱和吡啶原位吸附红外光谱等手段表征了催化剂. 结果表明, ZrO₂ 负载于 Si-MCM-41, Al-MCM-41 和 SiO₂ 后, 催化活性明显提高, 这归因于 ZrO₂ 与载体间存在强相互作用形成 Zr−O−Si 键, 使催化剂表面 Zr−OH 数量显著增多, Lewis 酸中心强度增强, 并出现 Brönsted 酸中心, 三种催化剂的活性高低次序是 5%ZrO₂/Si-MCM-41 > 5%ZrO₂/Al-MCM-41 > 5%ZrO₂/SiO₂. 而 5%ZrO₂/Al₂O₃ 和 5%ZrO₂/MgO 基本无催化活性, 可归因为 ZrO₂ 与 γ-Al₂O₃ 的弱相互作用使 5%ZrO₂/Al₂O₃ 的酸性与 γ-Al₂O₃ 类似, ZrO₂ 与 MgO 的强相互作用使 5%ZrO₂/MgO 基本无酸性.

关键词: 载体效应; Meerwein-Ponndorf-Verley 反应; 氧化锆; MCM-41 介孔分子筛; 苯甲醛

中图分类号: O643　　　**文献标识码**: A

Support Effect in Meerwein-Ponndorf-Verley Reduction of Benzaldehyde over Supported Zirconia Catalysts

ZHANG Bo*, TANG Minhui, YUAN Jian, WU Lei

Research Institute of Industrial Catalysis, Zhejiang University of Technology, Hangzhou 310014, Zhejiang, China

Abstract: A series of zirconia catalysts supported on Si-MCM-41 and Al-doped MCM-41 (Si/Al = 50) mesoporous molecular sieves, silica, γ-Al₂O₃, and MgO were prepared by the wet impregnation method. The catalytic activities of these materials in the Meerwein-Ponndorf-Verley reduction (MPV) of benzaldehyde with 2-propanol as reducing agent were investigated, and compared to that of hydrous zirconia. The materials were characterized by X-ray diffraction, nitrogen adsorption-desorption, X-ray photoelectron spectroscopy, UV-Vis diffuse reflectance spectroscopy, and Fourier transform infrared and thermal desorption of pyridine. Loading zirconia on Si-MCM-41, Al-MCM-41, and SiO₂ gave improved catalytic activity. This is attributed to a strong interaction of zirconia with the support to form Si–O–Zr bonds, which gave a significant increase in the amount of exposed Zr–OH groups and stronger Lewis acidity as well as an appearance of Brönsted acid sites. The activity of 5%ZrO₂/Si-MCM-41 was the highest, followed by those of 5%ZrO₂/Al-MCM-41 and 5%ZrO₂/SiO₂. However, 5%ZrO₂/Al₂O₃ and 5%ZrO₂/MgO gave very low catalytic activities. This is ascribed to that the acidities of 5%ZrO₂/Al₂O₃ and the γ-Al₂O₃ support were similar due to the weak interaction of zirconia with γ-Al₂O₃, and 5%ZrO₂/MgO had no acidity because of the strong interaction between zirconia and MgO.

Key words: support effect; Meerwein-Ponndorf-Verley reduction; zirconia; MCM-41 mesoporous molecular sieve; benzaldehyde

The selective hydrogenation of unsaturated carbonyl compounds is a very important step in the preparation of fine chemicals. The hydrogen-transfer approach, Meerwein-Ponndorf-Verley (MPV) reduction, can provide a better way to enhance the chemoselectivity to allylic alcohol than the traditional use of molecular hydrogen. Furthermore, unlike conventional hydrogenation, MPV reactions do not require an elaborate experimental setup or high pressure reactors. A typical reducing reagent is 2-propanol. Traditionally, the reaction is catalyzed homogeneously by metal alkoxides such as aluminum or titanium alkoxides [1]. It is generally accepted that the process proceeds via a six-membered cyclic transition-state complex in which the carbonyl group and the alcohol are both coordinated to a Lewis acid metal center, and a hydride transfer from the alcohol to the carbonyl group occurs. The homogenously catalyzed MPV reaction has some unavoidable drawbacks in that the catalyst is required in stoichiometric amounts and the separation of the catalyst is a tedious process. Hence, heterogeneous catalysts have gained increasing attention in recent years. These include magnesium oxides [2], hydrous zirconia [3,4], layered double hydroxides [5], Zr-β [6] and Sn-β zeolites [7], and metal alkoxides immobilized on mesoporous materials [8]. More than one MPV mechanisms over heterogeneous catalysts have been proposed depending on the particular catalyst used. The reduction of carbonyl compounds by hydrogen transfer has been hypothesized to occur at Lewis acid and/or Brönsted acid sites, basic sites, and acid-base pairs.

Zirconium-containing heterogeneous catalysts are reported to exhibit good resistance to the presence of water in addition to having good catalytic activity. Among these, the catalytic activity of hydrous zirconia is the lowest. However, hydrous zirconia has the advantages over other zirconium-containing catalysts of low cost and easy preparation. In order to improve the catalytic efficiency of metal oxides, the presence of a support can provide new means to tailor catalytic performance by altering the exposure of the active sites and modifying their nature by interaction with the support. In our previous study [9], the catalytic activities of pure MgO and MgO supported on activated carbon (AC), mesoporous molecular sieve MCM-41, silica, and γ-alumina in the MPV reduction of acetophenone with 2-propanol as reducing agent were investigated. The higher activity of MgO/AC to those of pure MgO and the other supported MgO catalysts was ascribed to the high surface area of AC and that there was no strong interaction of MgO with AC support, which favored the high dispersion of MgO on the surface of AC to form very small crystallites and increased the amount of basic sites on the surface of catalyst. On the other hand, the concentration of acetophenone near the active sites in the catalyst was increased because of the

π-electron interaction between the benzene ring in acetophenone and the graphite layer of the AC support, which also enhances the activity. However, the support effect on the catalytic performance of supported zirconia in the MPV reduction of carbonyl compounds has not been sufficiently addressed.

Due their textural and surface chemical features, silica [10], alumina [11], and magnesium oxide [12] are widely employed as catalyst supports. MCM-41 mesoporous molecular sieve is the most studied member of the M41S meso-structured family. It has some striking properties such as very high surface area, regular nano-sized pore structure, and adjustable heteroatom compositions. This material has been shown to be an excellent support for preparing supported catalysts with activity and selectivity superior to those of amorphous silica, alumina, and even zeolites [13]. In the present contribution, a series of zirconia supported on Si-MCM-41 and Al-doped MCM-41 (Si/Al = 50) mesoporous molecular sieves, silica, γ-alumina, and magnesium oxide were prepared by the wet impregnation method using zirconium nitrate as the precursor. The catalytic activities of these supported zirconia samples in the MPV reduction of benzaldehyde were investigated and compared to that of pure hydrous zirconia. The catalysts were characterized by X-ray diffraction (XRD), nitrogen adsorption-desorption, X-ray photoelectron spectroscopy (XPS), UV-Vis diffuse reflectance spectroscopy, and Fourier transform infrared (FT-IR) and thermal desorption of pyridine. The activities of the catalysts were correlated with the characterization results to gain a better insight into the support effect in the MPV reduction of benzaldehyde over supported zirconia catalysts.

1 Experimental

1.1 Preparation of catalysts

All the chemicals employed in the preparation of catalysts and reactions were analytical grade supplied by China Medicine (Group) Huadong Chemical Reagent Co. (Hangzhou, China). They were used as received without further purification.

Si-MCM-41 and Al-doped MCM-41 (Al-MCM-41, Si/Al = 50) mesoporous molecular sieves were synthesized by the hydrothermal method using methods that have been described elsewhere [13]. Sodium silicate and aluminium nitrate were selected as silica source and aluminium source, respectively. Cetyltrimethylammonium bromide (CTAB, C$_{16}$H$_{33}$(CH$_3$)$_3$NBr) was used as the structure-directing agent. The molar composition of the resulting gel was 1.0SiO$_2$:xAl$_2$O$_3$:0.2CTAB:120H$_2$O, where x was 0 for Si-MCM-41 and 0.01 for Al-MCM-41, respectively. The

resulting gels were crystallized in a Teflon-lined autoclave at 393 K for 3 d under autogenous pressure. The materials were recovered by filtration, washed with deionized water, dried at 383 K overnight, and then calcined in air at 823 K for 6 h in order to remove the template. Solid $Mg(OH)_2$ was obtained by precipitating 1 mol/L magnesium nitrate solution with 1 mol/L sodium hydroxide solution, and then calcined in the air at 773 K for 6 h to yield the support of magnesium oxide. Silica and γ-alumina were purchased from Shanghai Henye Chemical Plant (Shanghai, China).

Si-MCM-41, Al-MCM-41, silica, γ-alumina, and magnesium oxide supported zirconia catalysts were prepared by the wet impregnation method. A calculated amount of zirconium nitrate $(Zr(NO_3)_4 \cdot 5H_2O)$ was dissolved in deionized water, then the finely powered support was added to this solution. Excess water was evaporated on a water bath with continuous stirring. The resulting solid was dried in air at 383 K for 12 h, and further calcined in air at 573 K for 8 h. The zirconia content in the catalyst was maintained at 5%. The samples were labeled as $5\%ZrO_2$/Si-MCM-41, $5\%ZrO_2$/Al-MCM-41, $5\%ZrO_2/SiO_2$, $5\%ZrO_2/Al_2O_3$, and $5\%ZrO_2/MgO$. Hydrous zirconia, labeled as ZrO_2, was prepared by the precipitation of a 10% zirconium nitrate solution with excess 5 mol/L ammonium hydroxide. The precipitate was washed with deionised water and dried overnight at 373 K, then calcined at 573 K in air for 8 h. 573 K was reported to be the optimum calcination temperature of hydrous zirconia used in the MPV reduction of cinnamaldehyde and citral [3,4], so the catalysts in this work were calcined at this temperature.

1.2 Characterization of catalysts

Powder XRD measurements were carried on a Thermo ARL X'TRa diffractometer with Cu K_α radiation at a voltage of 40 kV and current of 40 mA. Samples were scanned in the 2θ range 1.0^o–70.0^o at a rate of 0.06^o/s. The textural properties of samples were determined from nitrogen adsorption-desorption isotherms obtained at 77 K on a Micromeritics ASAP 2010 M instrument. Prior to the measurement, the sample was degassed at 523 K for 5 h under high vacuum. The specific surface area was calculated from the adsorption isotherm by the Brunauer-Emmett-Teller (BET) method, while the mean pore diameter and cumulative pore volume were estimated by the Barrett-Joyner-Halenda (BJH) model using the desorption branch. XPS were performed with a Kratos ULTRA X photoelectron spectrometer equipped with a monochromatic Al K_α X-ray source (1486.6 eV). The C $1s$ peak of contaminant carbon at 284.8 eV was used as an internal standard for the correction of binding energies. The uncertainty in the determination of the binding energy values was estimated to

be 0.2 eV. UV-Vis spectra were collected in the 200−800 nm range on a Shimadzu 2550 spectrometer equipped a diffuse reflectance accessory at ambient temperature. $BaSO_4$ was the reference. Acid properties of samples were analyzed by FT-IR and thermal desorption of pyridine. Pyridine adsorption was performed in a conventional flow adsorption system using N_2 as carrier for 30 min. Physisorbed pyridine was removed by evacuation under vacuum for 30 min. Then, the thermal desorption was performed from room temperature to 573 K. The samples were analyzed in the range of 2000−1300 cm^{-1} using a Nicolet Nexus FTIR spectrometer. Band intensities were normalized by sample weight.

1.3 Catalytic experiments

The MPV reduction of benzaldehyde with 2-propanol was performed in a 25 ml three-necked round-bottom flask immersed in a thermostated bath and equipped with a condenser, a thermometer, and a magnetic stirrer. A reaction mixture of 3 mmol of the benzaldehyde and 60 mmol of 2-propanol was placed in the flask and refluxed with stirring at 355 K. The reaction was started by feeding 300 mg of freshly calcined catalyst into the mixture. After the reaction of 8 h, the catalyst was removed by filtration and reaction products were analyzed using a gas chromatograph (Agilent 6890N) equipped with a HP Innowax capillary column (30 m × 0.25 mm i.d.) and a flame ionization detector (FID). The various products were identified by GC/MS using a similar column and by comparison with calibration samples.

2 Results and discussion

2.1 XRD

The powder XRD patterns of $5\%ZrO_2$/Si-MCM-41 and $5\%ZrO_2$/Al-MCM-41 and the corresponding supports are displayed in Fig. 1(a). The small angle XRD patterns of Si-MCM-41 and $5\%ZrO_2$/Si-MCM-41 showed one major (100) reflection and two minor reflections corresponding to the (110) and (220) planes, indicating a highly ordered hexagonal pore structure [13]. The similarity in the intensity of the peaks of Si-MCM-41 and $5\%ZrO_2$/Si-MCM-41 revealed that the mesoporous structure was intact after the loading of zirconia. $5\%ZrO_2$/Al-MCM-41 and Al-MCM-41 also gave a typical XRD pattern for a 2D hexagonal mesophase. The decrease in the intensity of the diffraction peaks of Al-MCM-41 compared to Si-MCM-41 can be ascribed to that the substitution of Si^{4+} by Al^{3+} ions resulted in an alteration of the T−O−T bond angle and a slight decrease in the long range order of the mesostructure [13]. Upon loading zirconia into Al-MCM-41, a significant decrease in the
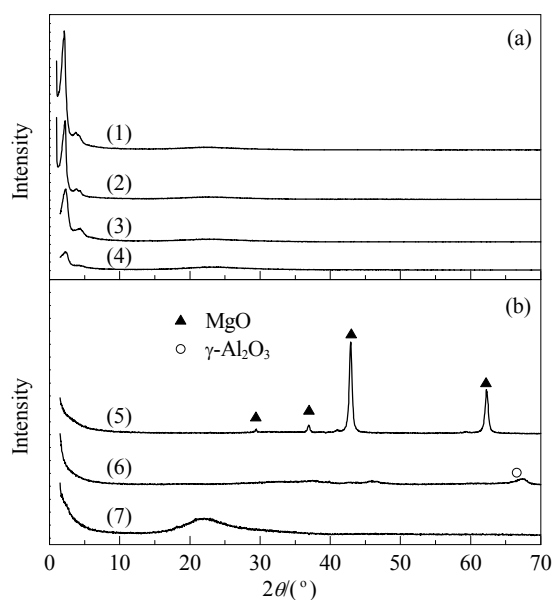
Fig. 1. XRD patterns of different samples. (1) Si-MCM-41; (2) 5%ZrO$_2$/Si-MCM-41; (3) Al-MCM-41; (4) 5%ZrO$_2$/Al-MCM-41; (5) 5%ZrO$_2$/MgO; (6) 5%ZrO$_2$/Al$_2$O$_3$; (7) 5%ZrO$_2$/SiO$_2$.

intensity of the [100] peak was visible in XRD pattern. This was due to the occurrence of disorder in the hexagonal structure of MCM-41. During the impregnation, the higher acidity of the zirconium nitrate solution (pH = 2−3) could have caused a transformation of some framework aluminum species of Al-MCM-41 into extra-framework octahedral aluminum species.

The XRD patterns of 5%ZrO$_2$/SiO$_2$, 5%ZrO$_2$/Al$_2$O$_3$, and 5%ZrO$_2$/MgO are shown in Fig. 1(b). 5%ZrO$_2$/SiO$_2$ exhibited a broad hump in the range of 2θ = 5°−40°, which was ascribed to the amorphous structure of the silica support [10]. 5%ZrO$_2$/Al$_2$O$_3$ and 5%ZrO$_2$/MgO presented weak diffraction peaks of γ-Al$_2$O$_3$ [11] and the characteristic peaks of MgO [2], respectively. No patterns of any bulk zirconia crystal phase [14] were observed in the high angle range for all supported ZrO$_2$ samples, implying that supported zirconia had an amorphous nature.

2.2　N$_2$ adsorption-desorption

The textural parameters of hydrous zirconia, support materials, and supported zirconia catalysts are summarized in Table 1. The N$_2$ adsorption-desorption isotherms (not shown) of Si-MCM-41, 5%ZrO$_2$/MCM-41, Al-MCM-41, and 5%ZrO$_2$/Al-MCM-41 samples exhibited Type IV isotherms with a completely reversible nature characteristic of solids with uniformly sized mesopores [13]. This indicated that the ordering of the hexagonal arrays of the mesopores in Si-MCM-41 and Al-MCM41 was not affected upon loading zirconia. The surface area and total pore volume

Table 1　Textural properties of different samples

Sample	BET surface area (m^2/g)	Mean pore diameter[a] (nm)	Pore volume[b] (cm^3/g)
ZrO$_2$	154	2.6	0.14
Si-MCM-41	1034	3.5	0.92
5%ZrO$_2$/Si-MCM-41	776	3.5	0.65
Al-MCM-41	998	3.8	0.95
5%ZrO$_2$/Al-MCM-41	737	3.3	0.65
SiO$_2$	176	7.7	0.34
5%ZrO$_2$/SiO$_2$	97	9.2	0.22
γ-Al$_2$O$_3$	208	10.6	0.55
5%ZrO$_2$/Al$_2$O$_3$	205	10.0	0.51
MgO	86	18.2	0.32
5%ZrO$_2$/MgO	112	6.6	0.18

[a]Calculated by the BJH method from the desorption isotherm.
[b]Total pore volume at p/p_0 = 0.99.

decrease from 1034 to 776 m^2/g and 0.92 to 0.65 cm^3/g or 998 to 737 m^2/g and 0.95 to 0.65 cm^3/g, respectively, after addition of 5% of zirconia into Si-MCM-41 or Al-MCM-41. This indicated the added zirconia was mainly located inside the Si-MCM-41 or Al-MCM-41 mesoporous channels. No change in the mean pore diameter between Si-MCM-41 and 5%ZrO$_2$/MCM-41 was observed. This result revealed that loaded zirconia was highly dispersed inside the mesopores of the Si-MCM-41 support. However, a slight decrease in the mean pore diameter from 3.8 to 3.3 nm was found when loading zirconia into Al-MCM-41, implying a lower dispersion of zirconia in 5%ZrO$_2$/Al-MCM-41 than in 5%ZrO$_2$/Si-MCM-41. This may be due to the probable formation of extra-framework aluminum species during the preparation of 5%ZrO$_2$/Al-MCM-41.

Compared with above samples, the silica, γ-Al$_2$O$_3$, MgO supports, and the corresponding supported zirconia samples had lower BET surface areas. Remarkable decreases in the BET surface area and total pore volume, as well as an increase in the mean pore diameter after the addition of zirconia into the silica support were observed. The surface area, pore volume, and mean pore diameter of 5%ZrO$_2$/Al$_2$O$_3$ were the same as the pure γ-Al$_2$O$_3$ support. The incorporation of zirconia into the MgO support caused an effective increase in the surface area and drastic decreases in the mean pore size and the pore volume. These results suggested the lower dispersion of zirconia in the silica, γ-Al$_2$O$_3$, and MgO supports than in the Si-MCM-41 and Al-MCM-41 supports.

2.3　XPS

All the supported zirconia samples and pure hydrous zirconia were investigated by XPS. The photoelectron peaks for Zr 3d for hydrous zirconia and various supported zirconia samples are shown in Fig. 2. Table 2 lists the binding
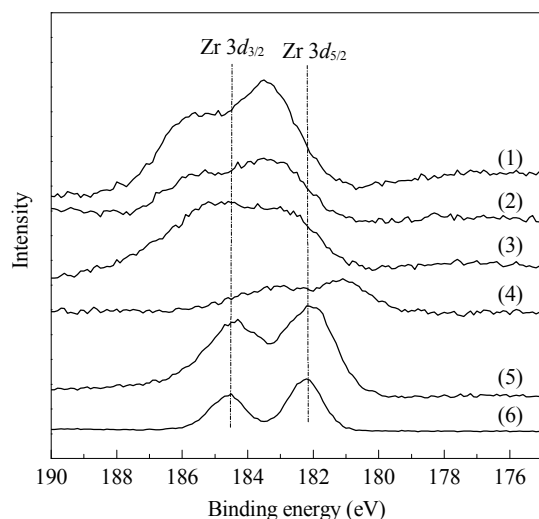
Fig. 2. XPS spectra of different samples. (1) 5%ZrO$_2$/Si-MCM-41; (2) 5%ZrO$_2$/Al-MCM-41; (3) 5%ZrO$_2$/SiO$_2$; (4) 5%ZrO$_2$/MgO; (5) 5%ZrO$_2$/Al$_2$O$_3$; (6) ZrO$_2$.

energies of the metal elements in the samples. Figure 2 shows the binding energies of the Zr 3d peaks of hydrous zirconia at ~182.2 and ~184.5 eV for Zr 3$d_{5/2}$ and Zr 3$d_{3/2}$ lines, respectively, which are in agreement with the value for Zr^{4+} in pure zirconia in the literature [14]. Compared to those of hydrous zirconia, there was an increase in the binding energies of the Zr 3$d_{5/2}$ and Zr 3$d_{3/2}$ core electron levels in the 5%ZrO$_2$/Si-MCM-41, 5%ZrO$_2$/Al-MCM-41, and 5%ZrO$_2$/SiO$_2$ samples. This shift towards higher values can be interpreted in terms of a strong interaction between zirconia and the support oxides, i.e., the formation of Si−O−Zr bonds [15]. There is enough evidence in the literature for an interaction between zirconia and other oxide supports [16,17]. The higher binding energy of Zr 3d indicated a higher positive charge on the Zr in the Si−O−Zr linkages, due to the smaller electronegativity of Zr than that of Si (Pauling values, Zr 1.4, Si 1.8) [16]. In addition, in comparison to hydrous zirconia, a trough between the Zr 3$d_{5/2}$ peak and Zr 3$d_{3/2}$ peak and a broadening of the Zr 3d peaks were seen for 5%ZrO$_2$/Al-MCM-41 and 5%ZrO$_2$/SiO$_2$. This can be attributed to the presence of more than

Table 2 XPS data of hydrous zirconia and various supported zirconia catalysts

Sample	Binding energy (eV)			
	Zr 3$d_{5/2}$	Si 2p	Al 2p	Mg 2p
ZrO$_2$	182.2	—	—	—
5%ZrO$_2$/Si-MCM-41	183.6	103.9	—	—
5%ZrO$_2$/Al-MCM-41	183.5	103.8	74.7	—
5%ZrO$_2$/SiO$_2$	183.0	103.6	—	—
5%ZrO$_2$/Al$_2$O$_3$	182.2	—	74.6	—
5%ZrO$_2$/MgO	181.1	—	—	49.0

one type of surface Zr^{4+} species with different chemical environments [17]. The extent of the Zr 3d peak broadening was less in the case of 5%ZrO$_2$/Si-MCM-41. This suggested that Zr^{4+} species had a more uniform chemical environment in the Si-MCM-41 support than in the Al-MCM-41 and silica supports. The results from the N$_2$ adsorption-desorption analysis indicated that the dispersion degree of zirconia in 5%ZrO$_2$/Si-MCM-41 was the highest, followed by those of 5%ZrO$_2$/Al-MCM-41 and 5%ZrO$_2$/SiO$_2$. It is a known fact that more Zr atoms can interact with the support to form Zr−O−Si bonds when the dispersion of zirconia is higher. Hence, it can be concluded that the amount of Si−O−Zr bonds in the three samples decreased in the sequence of 5%ZrO$_2$/Si-MCM-41 > 5%ZrO$_2$/Al-MCM-41 > 5%ZrO$_2$/SiO$_2$.

In the case of 5%ZrO$_2$/Al$_2$O$_3$, well resolved Zr 3d lines with high intensity were observed and the binding energies of Zr 3d were in agreement with those of pure hydrous zirconia. This indicated a weak interaction between zirconia and the γ-Al$_2$O$_3$ support.

From Fig. 2 and Table 2, a clear decrease in the binding energy of Zr 3d and an extensive broadening of the Zr 3d lines can be noted for the 5%ZrO$_2$/MgO sample compared to hydrous zirconia. This indicated that there was a stronger interaction between zirconia and the MgO support, perhaps with the formation of Mg−O−Zr bonds. The lower binding energy of Zr 3d indicated a lower positive charge density on the Zr atoms, which was attributed to the higher electronegativity of Zr than Mg (Pauling values, Zr 1.4, Mg 1.3) [16,18]. The observed extensive broading of the Zr 3d lines implied that some undefined ZrO$_x$ species were located on the surface of 5%ZrO$_2$/MgO.

For these supported zirconia samples, the binding energies of Si 2p (~103.7 eV), Al 2p (~74.6 eV), and Mg 2p (~49.0 eV) were essentially in agreement with the values of pure SiO$_2$, γ-Al$_2$O$_3$, and MgO reported in the literature. This was due to the significantly high content of the support (95%) [15−18].

2.4 UV-Vis

Figure 3 shows the UV-Vis spectra of supported zirconia samples with the hydrous zirconia spectrum as a reference. No feature characteristics of d−d transitions were displayed in the visible region (above 400 nm) in the electronic spectrum of all zirconia-containing samples [19], suggesting the d^0 configuration of the Zr^{4+} ions.

An intensive absorption band near 210 nm and a weak and broad shoulder extending from 270 to 390 nm were observed in the spectrum of hydrous zirconia. These adsorption bands can be assigned to O^{2-} (2p) to→Zr^{4+} (4d) charge transfer transitions. The absorption band at higher
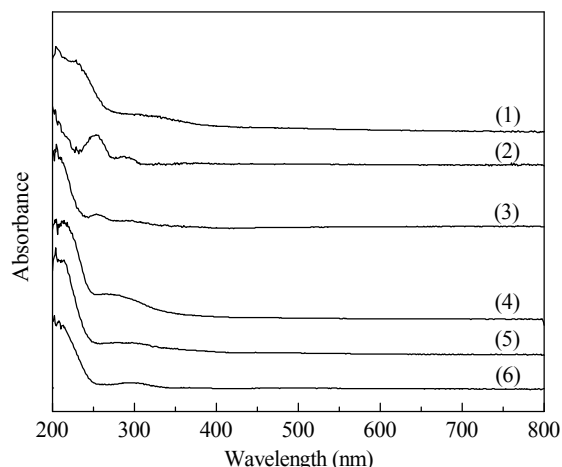
Fig. 3. UV-Vis spectra of different samples. (1) ZrO₂; (2) 5%ZrO₂/Si-MCM-41; (3) 5%ZrO₂/Al-MCM-41; (4) 5%ZrO₂/SiO₂; (5) 5%ZrO₂/Al₂O₃; (6) 5%ZrO₂/MgO.

energy was due to the normal energy gap transition in the bulk zirconia phase. The low energy shoulder was attributed to the $O^{2-} \rightarrow Zr^{4+}$ transitions from O^{2-} in low coordination sites at the surface of small particles [4,12,19]. Compared with hydrous zirconia, with the 5%ZrO₂/Si-MCM-41 sample, the intensity of the adsorption band below 230 nm was significantly decreased and the edge position of the low energy step was shifted to lower wavelength (high energy), while the intensity of the absorption band in the region of 230−270 nm was distinctly increased with the maximum adsorption at 250 nm. According to previous reports [19−21], in the UV-Vis spectra of Zr^{4+} species, eight-coordinated Zr^{4+} species (like those in cubic and tetragonal zirconia) are responsible for the adsorption in the 200−210 nm range, seven-coordinated Zr^{4+} species (like those in monoclinic zirconia) are associated to the absorption near 240 nm, and six-coordinated (octahedral) Zr^{4+} species give rise to the absorption located at 250−350 nm, i.e., the absorption by Zr^{4+} species shifts to higher wavelengths (lower energy) with the decrease of the coordination number of the Zr atoms. Hence, loading zirconia into the Si-MCM-41 support resulted in a clear decrease in the coordination number of the Zr species. This can be attributed to the interaction of high dispersed zirconia with the surface of the Si-MCM-41 support to form Zr−O−Si bonds during the calcination. It was reported through characterization by extended X-ray absorption fine structure (EXAFS) [22] that monolayer-like dispersion of zirconia on the silica MCM-41 support calcined at 673 K showed a decreased Zr−O coordination as compared to that of the bulk zirconia phase. This was ascribed to the partial dehydration of zirconium hydroxide to anchor it to the silica surface [22]. Compared with 5%ZrO₂/Si-MCM-41, 5%ZrO₂/Al-MCM-41 showed a more intense absorption edge below 240 nm and a weaker

absorption band at 250 nm. This indicated less decrease in the coordination number of the Zr species in 5%ZrO₂/Al-MCM-41 than in 5%ZrO₂/Si-MCM-41. This could be due to the lower dispersion of zirconia in the former. In contrast to 5%ZrO₂/Si-MCM-41 and 5%ZrO₂/Al-MCM-41, the UV-Vis spectra profiles of 5%ZrO₂/SiO₂, 5%ZrO₂/Al₂O₃, and 5%ZrO₂/MgO resembled that of hydrous zirconia, but the edge position of the low energy absorption was shifted to a lower wavelength (higher energy) from 270 to 250 nm. In addition, the intensity of the low energy shoulder of 5%ZrO₂/SiO₂ was larger than that of 5%ZrO₂/Al₂O₃, 5%ZrO₂/MgO, and hydrous zirconia. These results indicated that the coordination of the Zr^{4+} species in 5%ZrO₂/Al₂O₃ and 5%ZrO₂/MgO was basically like that in pure hydrous zirconia, while 5%ZrO₂/SiO₂ has more Zr^{4+} species with a lower Zr−O coordination number. Hence, the amount of Zr^{4+} species with a lower Zr−O coordination number in 5%ZrO₂/Si-MCM-41 was the highest, followed by those of 5%ZrO₂/Al-MCM-41 and 5%ZrO₂/SiO₂. This was in agreement with the order of amount of Si−O−Zr bonds in these samples. The amounts of Zr^{4+} species with a lower Zr−O coordination number in 5%ZrO₂/Al₂O₃ and 5%ZrO₂/MgO were the lowest.

2.5 FT-IR and thermal desorption of pyridine

The acid properties of the samples were analyzed by FT-IR and thermal desorption of pyridine. Only three weak infrared bands at 1597, 1446, and 1577 cm⁻¹ were observed for the Si-MCM-41 and silica supports (not shown). These were ascribed to hydrogen bonded pyridine, where the −OH groups were not acidic enough to transfer their proton to pyridine (very weak interaction) [23]. This suggested a relatively weak surface acidity for the Si-MCM-41 and silica supports. Besides these three bands, the Al-MCM-41 support presented another very weak peak at 1490 cm⁻¹ (not shown here), assigned to chemisorbed pyridine on either Lewis or Brönsted acid sites [24]. This indicated that the substitution of a small amount of Si^{4+} by Al^{3+} ions (Si/Al = 50) in Si-MCM-41 caused a slight increase in the acidity.

Figure 4 shows the FT-IR spectra of pyridine adsorption on hydrous zirconia and supported zirconia samples evacuated at room temperature, 373 K, and 423 K. In Fig. 4(a), only two very weak adsorption peaks were observed on hydrous zirconia at 1443 and 1603 cm⁻¹, which were attributed to coordinated pyridine species on Lewis acid sites [22,23]. This showed that pure hydrous zirconia possessed few Lewis acid sites. For 5%ZrO₂/Si-MCM-41, 5%ZrO₂/Al-MCM-41, and 5%ZrO₂/SiO₂ as compared to the corresponding supports and pure zirconia, the intensities of the adsorption bands at 1597, 1577, and 1446 cm⁻¹ were significantly increased. This suggested an effective increase in
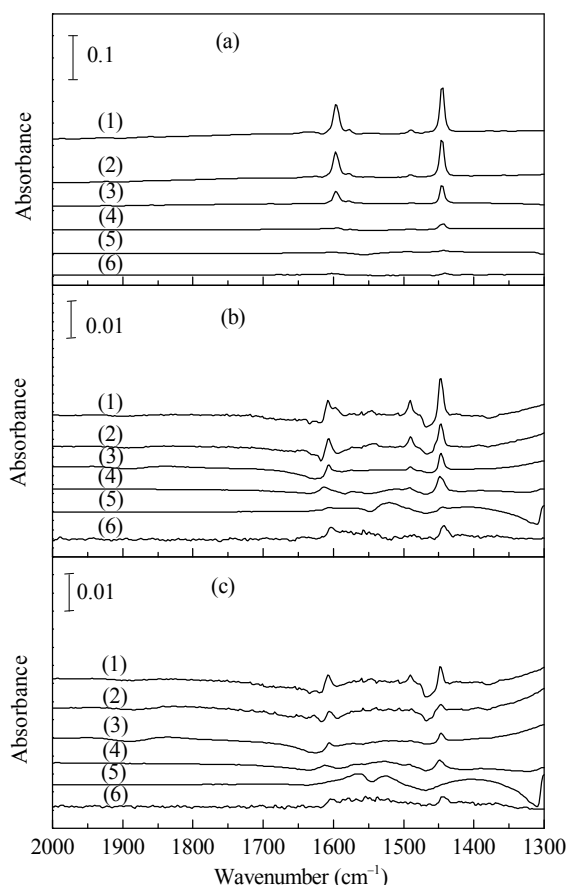
Fig. 4. Pyridine-FT-IR spectra of samples after desorption at room temperature (a), 373 K (b), and 423 K (c). (1) 5%ZrO$_2$/Si-MCM-41; (2) 5%ZrO$_2$/Al-MCM-41; (3) 5%ZrO$_2$/SiO$_2$; (4) 5%ZrO$_2$/Al$_2$O$_3$; (5) 5%ZrO$_2$/MgO; (6) ZrO$_2$.

the amount of −OH groups on the surface interacting with pyridine by hydrogen bonding. This was attributed to the appearance of plentiful Zr−OH groups due to the dispersion of zirconia on the surface of the supports and the higher coordination number of Zr with respect to Si [25]. The intensities of the above desorption bands decrease in the order of 5%ZrO$_2$/Si-MCM-41 > 5%ZrO$_2$/Al-MCM-41 > 5%ZrO$_2$/SiO$_2$, suggesting that the amount of Zr−OH groups in the three samples decreases in the same order. In addition, bands at 1638, 1628, 1545, and 1490 cm^{-1} were observed for 5%ZrO$_2$/Si-MCM-41and 5%ZrO$_2$/ Al-MCM-41, and a weak band at 1490 cm^{-1} was found for 5%ZrO$_2$/SiO$_2$. The comparison with literature data suggested that the bands at 1638 and 1545 cm^{-1} were due to pyridinium ion on Brönsted acid sites and the band at 1628 cm^{-1} was attributed to coordinated pyridine species on Lewis acid sites [13,23−26]. It is clear that both Brönsted acid and Lewis acid sites interacting strongly with pyridine were present on these supported samples. This result means that the acidities of these samples were stronger than those of pure zirconia and the corresponding supports. This was probably associ-

ated with the interaction of zirconia with the supports and the coordination number of Zr^{4+} species. It had been reported [27,28] that on monoclinic zirconia, in which the Zr^{4+} cation is heptacoordinated, there exists both Brönsted acid and Lewis acid sites, while only Lewis acid sites were detected by IR measurement after pyridine adsorption on tetragonal zirconia in which the Zr^{4+} cation is octacoordinated. Furthermore, the surface acid site density is higher on monoclinic zirconia than on tetragonal zirconia. On the other hand, for these supported zirconia samples, the interface between zirconia and support can be considered a silica-zirconia mixed oxide due to the formation of Si−O−Zr bonds. According to Tanabe's hypothesis [29,30], acidity generation in a binary oxide is caused by an excess of negative or positive charge. For the silica-zirconia mixed oxide, the Brönsted acidity was related the presence of an excess of negative charge due to that the coordination numbers of Si (4) and Zr (8, 7, or 6) elements are different but the oxygen anions adopt the coordination number of the host oxide (in silica-rich region). The higher positive charge on Zr in the Si−O−Zr linkage, indicated by the XPS analysis, implied more Lewis acid sites on zirconium in the silica-zirconia mixed oxides.

Comparing Fig. 4(a)−(c), for 5%ZrO$_2$/Si-MCM-41, 5%ZrO$_2$/Al-MCM-41, and 5%ZrO$_2$/SiO$_2$, upon outgassing at increasing temperatures, the intensities of all the bands decreased. This was more pronounced for the bands at 1597 and 1446 cm^{-1}, confirming that hydrogen bonded pyridine was very weakly held on the supports. At the same time, an appearance of a band at 1609 cm^{-1} and a shift of the band from 1446 to 1448 cm^{-1} were found. The two new bands were assigned to coordinated pyridine on Lewis acid sites [26], overlapped by the bands at 1597 and 1446 cm^{-1} at room temperature. It was observed that the bands corresponding to Lewis acid sites were stronger and more abundant than those of Brönsted acid sites, indicating the amount of Lewis acid sites was much higher than that of Brönsted acid sites. The bands at 1609, 1490, and 1448 cm^{-1} still remained while the bands assigned to Brönsted acid sites had almost diminished at 423 K, implying that the strength of the Lewis acid sites was stronger than that of the Brönsted acid sites. On the other hand, the higher wavenumbers of the Lewis acid sites for these samples compared to those observed for pure zirconia meant that the strength of the Lewis acid sites was stronger.

The intensity of the bands attributed to Brönsted and Lewis acid sites in the spectra of 5%ZrO$_2$/Si-MCM-41 was the highest, followed by those of 5%ZrO$_2$/Al-MCM-41 and 5%ZrO$_2$/SiO$_2$, suggesting that the amount of Brönsted and Lewis acid sites followed the same order, which agreed well with the order of amounts of Si−O−Zr bonds and Zr species with a lower coordination number.

From Fig. 4(a)−(c), weak bands at 1614, 1595, 1490, and 1445 cm^{-1} were observed for 5%ZrO₂/Al₂O₃ at room temperature. With the increase of outgassing temperature, the band at 1595 cm^{-1} rapidly disappeared while the band at 1444 cm^{-1} shifted to 1448 cm^{-1}. The bands at 1595 and 1445 cm^{-1} were attributed to hydrogen bonded pyridine. The intensities of these were significantly lower in comparison with those of 5%ZrO₂/Si-MCM-41, 5%ZrO₂/Al-MCM-41, and 5%ZrO₂/SiO₂. The bands at 1614, 1490, and 1448 cm^{-1} were assigned to pyridine adsorbed on Lewis acid sites [24−30]. The wavenumbers of these bands were slightly higher than those observed for pure zirconia but close to those reported for the Lewis acid sites on γ-Al₂O₃ [31,32]. No Brönsted acid sites were observed, as revealed by the absence of the pyridinium bands at about 1630 and 1540 cm^{-1}. In the literature [31,32], it was reported that γ-Al₂O₃ only possesses Lewis acidity. This indicated that the acidity of 5%ZrO₂/Al₂O₃ is basically similar to that of the γ-Al₂O₃ support. XPS results confirmed there was a quite weak interaction between zirconia and the γ-Al₂O₃ support. Hence, the acidity of 5%ZrO₂/Al₂O₃ would resemble that of a mechanical mixture of zirconia and γ-Al₂O₃. The Lewis acid sites and surface −OH groups of 5%ZrO₂/Al₂O₃ were mainly due to the γ-Al₂O₃ support, due to the small loaded amount (5%) and low dispersion of zirconia in the catalyst.

In comparison with the other supported zirconia samples and hydrous zirconia, almost no adsorption band can be found in the IR spectrum of pyridine adsorption for 5%ZrO₂/MgO. It implied negligible acidity for 5%ZrO₂/MgO. This can be explained by the strong interaction between zirconia and the MgO support as confirmed by XPS results, which lead to the decrease of the positive charge of Zr when in the Mg−O−Zr linkages [23,33].

2.6 Catalytic studies

During the MPV reduction of benzaldehyde using 2-propanol as reducing agent, benzaldehyde is reduced to benzyl alcohol and 2-propanol is oxidized to acetone. Table 3 shows the conversion of benzaldehyde and selectivity for benzyl alcohol over hydrous zirconia and the various supported zirconia catalysts. All the supports were inactive (conversion of benzaldehyde < 2%, not listed). Hydrous zirconia showed a low conversion of benzaldehyde (33.7%) and quite high selectivity for benzyl alcohol (99.2%) after a reaction of 8 h. The conversion of benzaldehyde was significantly enhanced upon loading zirconia into Si-MCM-41, Al-MCM-41, and SiO₂, and at the same time, the selectivity for benzyl alcohol was maintained. The activities of the three catalysts increased in the order 5%ZrO₂/SiO₂ (51.5%) < 5%ZrO₂/Al-MCM-41 (56.1%) < 5%ZrO₂/Si-MCM-41 (88.5%). In contrast, loading zirconia into γ-Al₂O₃ or MgO

Table 3 MPV reduction of benzaldehyde over hydrous zirconia and supported zirconia

Sample	Conversion (%)	Selectivity for benzyl alcohol (%)
ZrO₂	33.7	99.2
5%ZrO₂/Si-MCM-41	88.5	99.1
5%ZrO₂/Al-MCM-41	56.1	99.5
5%ZrO₂/SiO₂	51.5	99.8
5%ZrO₂/Al₂O₃	3.9	96.2
5%ZrO₂/ MgO	3.3	97.8

Reaction conditions: benzaldehyde 3 mmol, 2-propanol 60 mmol, catalyst 300 mg , 355 K, 8 h.

resulted in a dramatic fall of benzaldehyde conversion (< 5%) and a slight decrease of benzyl alcohol selectivity. The activities of 5%ZrO₂/Al₂O₃ and 5%ZrO₂/MgO were closed to those of the γ-Al₂O₃ and MgO supports.

Hydrous zirconia is an active catalyst for the MPV reduction of cinnamaldehyde and citral using 2-propanol as the hydrogen donor [5,6]. The pretreatment temperature of hydrous zirconia has a big effect on the activity. The oxide calcined at 573 K was the most active, and above it, the catalytic activity decreased with calcination temperature. Chuah et al. [3,4] suggested that, besides surface area and porosity, the exposed hydroxyl groups of hydrous zirconia have a big influence on activity. They proposed that hydroxyl groups act as sites for ligand exchange with 2-propanol to form 2-propoxide on the catalyst. The carbonyl compound coordinates to the zirconium metal center. This activates the carbonyl group and initiates a hydride transfer from 2-propoxide to the carbonyl through a cyclic six-membered transition state, as has been proposed for beta zeolite. Acetone is formed and subsequent alcoholysis leads to the product and regeneration of the active catalyst. According to above mechanism, the increase in the number of exposed Zr−OH groups and strength of Lewis acidity (Zr^{4+} center) favor the improvement of catalytic activity. Urbano et al. [34] investigated the catalytic activity of zirconia modified with boron and alkaline-earth metal calcined at 673 K in the MPV reduction of cinnamaldehyde with 2-propanol. They found that an increase of surface hydroxyl groups of the catalyst led to an enhancement of its activity, and proton (Brönsted) acid sites of medium-high strength were the most catalytically active sites, while a potential contribution of Lewis acid sites cannot be ruled out. They also reported that the solids with an increased proportion of weak acid sites interacting with pyridine by hydrogen bonding or a high density of basic sites were much less active.

The comparison of the acidity characterization and MPV reduction of benzaldehyde test results showed that the catalytic activity is closely related to surface acidity. The higher

catalytic activities of 5%ZrO$_2$/Si-MCM-41, 5%ZrO$_2$/Al-MCM-41, and 5%ZrO$_2$/SiO$_2$ than that of hydrous zirconia can be attributed to a significant increase in the amount of surface Zr−OH groups and the strengthening of Lewis acidity, as well as the appearance of Brönsted acid sites. For these three catalysts, the activity increased with the amount of surface Zr−OH groups, Brönsted and Lewis acid sites. The very low activity of 5%ZrO$_2$/Al$_2$O$_3$ can be attributed to that its surface acidity resembled that of the γ-Al$_2$O$_3$ support. The very low activity of 5%ZrO$_2$/MgO can be ascribed to the absence of acidity of its surface. This is different from the results of Urbano et al. [34] that a significant increase in the amount of weak acid sites, i.e. Zr−OH groups interacting with pyridine by hydrogen bonding, favors the enhancement of catalytic activity. This could be due to the differences in the preparation of catalysts of the two works.

3 Conclusions

The MPV reduction of benzaldehyde with 2-propanol was carried out over a series of zirconia catalysts supported on Si-MCM-41, Al-doped MCM-41 (Si/Al = 50) mesoporous molecular sieves, silica, γ-Al$_2$O$_3$, and magnesium oxide, and compared to that of pure hydrous zirconia. Differences in catalytic activities observed for the supported zirconia catalysts with respect to pure hydrous zirconia indicated that the carrier affected the activity. The interaction of zirconia with the support has an important role in the surface acidity of the supported zirconia catalysts, which correlated strongly with the catalytic activity. For an interaction between zirconia and the support that favors a significant increase in the amount of surface Zr−OH groups and the strengthening of Lewis acidity, and appearance of Brönsted acid sites, there is enhancement of catalytic activity.

References

1 Ruiz J R, Jimenez-Sanchidrián C. *Current Org Chem*, 2007, **11**: 1113
2 Gliński M. *Appl Catal A*, 2008, **349**: 133
3 Zhu Y Z, Liu S H, Jaenicke S, Chuah G. *Catal Today*, 2004, **97**: 249
4 Liu S H, Jaenicke S, Chuah G K. *J Catal*, 2002, **206**: 321
5 石能富, 张波, 徐春雷, 张新波, 陈银飞, 葛忠华. 高校化学工程学报 (Shi N F, Zhang B, Xu Ch L, Zhang X B, Chen Y F, Ge Zh H. *J Chem Eng Chin Univ*), 2011, **25**: 61
6 Zhu Y Z, Chuah G K, Jaenicke S. *J Catal*, 2006, **241**: 25
7 Samuel P P, Shylesh S, Singh A P. *J Mol Catal A*, 2007, **266**: 11
8 Zhu Y Z, Jaenicke S, Chuah G K. *J Catal*, 2003, **218**: 396
9 徐春雷, 张波, 袁剑, 卢晗锋, 陈银飞, 葛忠华. 化学学报 (Xu Ch L, Zhang B, Yuan J, Lu H F, Chen Y F, Ge Zh H. *Acta Chim Sin*), 2011, **69**: 368
10 Busto M, Lovato M E, Vera C R, Shimizu K, Grau J M. *Appl Catal A*, 2009, **355**: 123
11 胡胜华, 薛明伟, 陈慧, 孙寅璐, 沈俭一. 催化学报 (Hu S H, Xue M W, Chen H, Sun Y L, Shen J Y. *Chin J Catal*), 2011, **32**: 917
12 Ciuparu D, Ensuque A, Bozon-Verduraz F. *Appl Catal A*, 2007, **326**: 130
13 Liu D P, Quek X Y, Cheo W N E, Lau R, Borgna A, Yang Y H. *J Catal*, 2009, **266**: 380
14 Chen C-L, Cheng S F, Lin H-P, Wong S-T, Mou C-Y. *Appl Catal A*, 2001, **215**: 21
15 Damyanova S, Petrov L, Centeeno M A, Grange P. *Appl Catal A*, 2002, **224**: 271
16 Reddy B M, Chowdhury B, Smirniotis P G. *Appl Catal A*, 2001, **211**: 19
17 Reddy B M, Sreekanth P M, Yamada Y, Kobayashi T. *J Mol Catal A*, 2005, **227**: 81
18 Wakiya N, Kuroyanagi K, Xuan Y, Shinozaki K, Mizutani N. *Thin Solid Films*, 2000, **372**: 156
19 López E F, Escribano V S, Panizza M, Carnasciali M M, Busca G. *J Mater Chem*, 2001, **11**:1891
20 Zhao J, Yue Y H, Hua W M, He H Y, Gao Z. *Appl Catal A*, 2008, **336**: 133
21 Chary K V R, Ramesh K, Naresh D, Ramana Rao P V, Ramachandra Rao A, Venkat Rao V. *Catal Today*, 2009, **141**: 187
22 Wang J-H, Mou C-Y. *Microporous Mesoporous Mater*, 2008, **110**: 260
23 Ordomsky V V, Sushkevich V L, Ivanova I I. *J Mol Catal A*, 2010, **333**: 85
24 Ahmed M A. *Fuel Process Technol*, 2011, **92**: 1121
25 Flego C, Carluccio L, Rizzo C, Perego C. *Catal Commun*, 2001, **2**: 43
26 Garg S, Soni K, Muthu Kumaran G, Bal R, Gora-Marek K, Gupta J K, Sharma L D, Murali Dhar G. *Catal Today*, 2009, **14**: 125
27 Zhang W, Tay H L, Lim S S, Wang Y S, Zhong Z Y, Xu R. *Appl Catal B*, 2010, **95**: 93
28 Zhao Y B, Li W, Zhang M H, Tao K Y. *Catal Commun*, 2002, **3**: 239
29 Rodríguez Avendaño R G, De Los Reyes J A, Viveros T, Montoya De La Fuente J A. *Catal Today*, 2009, **148**: 12
30 Gervasini A, Messi C, Flahaut D, Guimon C. *Appl Catal A*, 2009, **367**: 113
31 Li J C, Xiang L, Xu F, Wang Z W, Wei F. *Appl Surf Sci*, 2006, **253**: 766
32 Scirè S, Crisafulli C, Maggiore R, Minicò S, Gavagno S. *Appl Surf Sci*, 1998, **136**: 311
33 García V, Fernández J J, Ruíz W, Mondragón F, Moreno A. *Catal Commun*, 2009, **11**: 240
34 Urbano F J, Aramendia M A, Marinas A, Marinas J M. *J Catal*, 2009, **268**: 79